



Please cite the Published Version

Silva, Luiz RG, Stefano, Jéssica S, Crapnell, Robert D , Banks, Craig E  and Janegitz, Bruno C (2023) Additive manufactured microfluidic device for electrochemical detection of carbendazim in honey samples. *Talanta Open*, 7. p. 100213. ISSN 2666-8319

DOI: <https://doi.org/10.1016/j.talo.2023.100213>

Publisher: Elsevier

Version: Published Version

Downloaded from: <https://e-space.mmu.ac.uk/631851/>

Usage rights:  [Creative Commons: Attribution-Noncommercial-No Derivative Works 4.0](#)

Additional Information: This is an Open Access article which appeared in *Talanta Open*, published by Elsevier

Enquiries:

If you have questions about this document, contact openresearch@mmu.ac.uk. Please include the URL of the record in e-space. If you believe that your, or a third party's rights have been compromised through this document please see our Take Down policy (available from <https://www.mmu.ac.uk/library/using-the-library/policies-and-guidelines>)



Additive manufactured microfluidic device for electrochemical detection of carbendazim in honey samples

Luiz R.G. Silva^a, Jéssica S. Stefano^a, Robert D. Crapnell^b, Craig E. Banks^{b,*},
Bruno C. Janegitz^{a,*}

^a Laboratory of Sensors, Nanomedicine, and Nanostructured Materials, Federal University of São Carlos, Araras, São Paulo, Brazil

^b Faculty of Science and Engineering, Manchester Metropolitan University, Chester Street, Manchester, M1 5GD, UK

ARTICLE INFO

Keywords:

Additive manufacturing
Crops
Agrochemical
3d printing
Electrochemistry
sensing

ABSTRACT

The use of pesticides is one of the primary means of protecting crops. However, this class of compounds can be highly toxic to the environment and humans. In this aspect, developing analytical devices for monitoring pesticides such as carbendazim in food sources is of paramount importance. Thus, the present work presents the application of a paper-based microfluidic device coupled to an additive manufactured platform and electrochemical sensors (produced from lab-made conductive filaments based on carbon black) for the sustainable detection of carbendazim in honey samples. The microfluidic system presented satisfactory results for the analysis of carbendazim, in the linear range from 0.5 to 40.0 $\mu\text{mol L}^{-1}$ with a LOD of 0.09 $\mu\text{mol L}^{-1}$. The recovery test performed in honey samples showed values ranging between 92.4 and 108.8%. According to the results, the proposed microfluidic device demonstrated a good potential for detecting carbendazim in real samples, with the advantages of employing sustainable and renewable materials.

1. Introduction

The application of pesticides as crop defenders is widely used in agriculture and other practices [1]. However, even though pesticides play an important role in protecting crops, their excessive use is one of the main environmental problems faced [1,2]. Many pesticides are highly toxic to humans, among them carbendazim. Carbendazim (CBZ) is classified as a highly dangerous pesticide by the World Health Organization and has possible carcinogenic effects on humans [1,3]. In addition, it is classified in the priority list of chemicals that disrupt the endocrine system according to the European Union. Carbendazim is banned in several countries of the European Union and the USA due to its high-risk rate [1,4]. However, in some European countries, and countries like China and Brazil, this compound is still widely used [1].

The presence of CBZ residues in products is extremely worrying due to the high risk of intoxication [4,5]. In Brazil, a highly commercialized product such as honey has current legislation for the maximum control of CBZ residues, and the maximum limit of CBZ residues allowed in honey is 0.52 $\mu\text{mol L}^{-1}$ [6]. Considering this, the development of new devices and analytical methods for the quantification of this compound in different and complex samples is of great importance and relevance

for environmental and food monitoring. In this context, electrochemical methods and devices stand out due to their extremely attractive qualities, especially when linked to the use of 3D technology.

Electrochemical techniques have outstanding qualities such as the ability to provide fast responses when compared to other analytical techniques, require low amounts of samples and reagents, no specialized operators are needed, and can be eco-friendly, depending on the apparatus and electrodes employed [7–9]. In this sense, the manufacture of additive manufactured electrochemical sensors and platforms can provide the required electroanalytical apparatus from sustainable materials, as is the case of polylactic acid (PLA), which is a biodegradable polymer [10–12]. The use of 3D printing provides additional advantages, such as low-cost, scalable, and automatized production of sensors and apparatus, and the possibility to obtain objects with the most varied shapes and designs, ideal for the construction of sensing and fluidic platforms [11,13].

Microfluidic devices have shown great efforts to be the industry's most distinguished domain for chemical analysis [14–16]. A microfluidic device can promote the uniform distribution of a single aliquot of the sample with reduced volumes in the scale of nanoliters to microliters [14]. In addition, paper can be used as a distribution agent and

* Corresponding authors.

E-mail addresses: c.banks@mmu.ac.uk (C.E. Banks), brunocj@ufscar.br (B.C. Janegitz).

<https://doi.org/10.1016/j.talo.2023.100213>

Received 23 February 2023; Received in revised form 15 March 2023; Accepted 1 April 2023

Available online 2 April 2023

2666-8319/© 2023 The Authors. Published by Elsevier B.V. This is an open access article under the CC BY-NC-ND license (<http://creativecommons.org/licenses/by-nc-nd/4.0/>).

distribution channel for the sample to travel through, reaching the electrodes in the case of electrochemical sensing [14]. In this way it is possible to create an additive manufactured microfluidic device in association with paper, thus providing a device that makes use of sustainable, recyclable, and renewable materials for simple and fast electrochemical analysis of compounds of interest.

In the literature, there is a range of works that explore the use of electrochemical sensors for CBZ detection. Among the different sensors found, it can be mentioned carbon paste electrode (CPE) [17], glassy carbon electrode (GCE) [18], and boron-doped diamond electrode (BDD) [19]. However, these electrodes are mostly highly modified, and only a few electrodes report a simpler application such as the one presented by the work of Raymundo-Perreira et al., 2020 [20], which reports the detection of CBZ in wine with a disposable commercial electrode. Another recently published work is that of Martins et al., 2023 [21] which detects CBZ on the skin of apples and cabbage with disposable electrodes based on carbon ink. However, regarding the use of additive-manufactured sensors, only one work, developed by our research group has been published involving the detection of CBZ with additive-manufactured electrochemical sensors, using graphite and PLA-based sensor [22]. To our knowledge, there are no reports in the literature regarding the development of 3D printed CB-based sensors for the detection of pesticides such as CBZ. Furthermore, the use of microfluidic devices manufactured entirely in 3D for the electrochemical detection of CBZ or other types of pesticides is not yet reported in the literature. Thus, producing microfluidic 3D printed devices for pesticide detection (CBZ) is a hot topic with great potential, since it adds several advantages and positive aspects, mainly in terms of the use of low volume of samples for analysis and the low cost of the material. Furthermore, by using paper as a fluidic channel, the operator can reduce the direct contact with the solution or sample contaminated with the pesticide.

Therefore, the present work presents the manufacture of the first fully additive manufactured (3D-printed) microfluidic platform, coupled with a paper-based distribution channel for the electrochemical analysis of CBZ in honey samples. The electrochemical sensors were completely additively manufactured from conductive filaments produced in the laboratory based on PLA and carbon black.

2. Experimental

2.1. Reagents and solutions

Ultrapure water from a Milli-Q Plus system (Millipore Corporation®, Germany) with a resistivity higher than 18.0 MΩ cm was used to prepare all solutions. Carbendazim (98% w/w) and ferrocemethanol (FcMeOH) (99% w/w) were obtained from Sigma-Aldrich (St. Louis, USA), sodium hydroxide (NaOH) (99% w/w) from Vetec (Rio de Janeiro, Brazil). A 0.1 mol L⁻¹ Britton-Robinson (BR) buffer (pH 4.0) was used as a supporting electrolyte and was prepared from a mixture of boric acid (99.5% w/w), from Vetec, and phosphoric (85% v/v) and acetic (99.7% v/v) acids from Dinamica (Indaiatuba, Brazil). The stock solution of CBZ (5.0 mmol L⁻¹) was freshly prepared before experiments by dissolution in 0.1 mol L⁻¹ sulfuric acid (85% v/v) from Dinamica (Indaiatuba, Brazil). For the construction of the calibration curve of CBZ, the stock solution was diluted in different concentrations of BR buffer (pH 4.0).

2.2. Instrumental and apparatus

A SETH3D S3 3D printer (Campinas, Brazil) was used for printing the structures and electrodes employed in this work, controlled by the software Simplify 3DTM for the obtention of the structures by the fused deposition modeling (FDM) technique. A Filmaq3D® extruder (Curitiba, Brazil) was used for the extrusion of the obtained composites.

All electrochemical tests were carried out with the aid of a portable potentiostat μSTAT i-400 (Metrohm DropSens®, Spain) controlled by a

laptop, with Windows 10® operating system (Intel core i5 processor and 8.0 GB RAM), through the Dropview 8400® software. For the characterization of the materials, scanning electron microscopy (SEM) from Thermo Fisher Scientific model Prisma E with ColorSEM Technology and integrated energy-dispersive X-ray spectroscopy was used for the acquirement of SEM images. Contact angle images were obtained using a homemade apparatus, described in the literature [23]. To calculate the contact angle in the obtained images, the free software Blender® was used.

2.3. Composite filament, CB-PLA electrodes, and fluidic device

The electrodes employed in this work were additively manufactured from a lab-made composite filament composed of PLA and carbon black (CB) (28.5% wt.), which was called CB-PLA, obtained following a previous work from our research group [10,24]. For this, an adequate amount of pellets of PLA was dissolved in a mixture of solvents (acetone/chloroform, 4:1 v/v), with subsequent incorporation of CB. This process was carried out in a reflux system, under constant magnetic stirring and at a temperature of 70 °C. After 3 h, a recrystallization process was performed using ethanol, followed by filtration. The composite obtained was dried in the oven at 50 °C for 12 h, and finally, the extrusion of the composite was performed at 180 °C to provide the conductive filaments based on CB. PLA used to manufacture the composite filaments was obtained as pellets *in nature*, from 3DLAB (Minas Gerais, Brazil) and Carbon black (VULCAN® XC-72R) from Cabot (São Paulo, Brazil).

The microfluidic device was additive manufacturing (3D-printed) using non-conductive PLA filaments (from 3DLAB, Minas Gerais, Brazil). Fig. 1 presents a summary illustration presents a schematic of the steps involved, together with the dimensions of the microfluidic device. The devices were printed on a rectangular mold with a width of 2 cm, a height of 10 cm, and a thickness of 1.5 cm, with the mold for the allocation of the filter paper responsible for the fluidic channel to the solution. In addition, the microfluidic system contained a mold for fitting the three electrodes (working, counter, and pseudo reference) so that they can be placed on the fluidic paper channel and a circular waste reservoir with a diameter of 3.5 cm is at the end of the fluidic paper. A timelapse of the 3D printing of the fluidic device and how to apply it can be found in the supplementary material. Also, Fig. S1 illustrates the scheme of the drop (solution) deposition process in the fluidic device.

2.4. Voltammetric analysis

To perform the square wave voltammetry (SWV) analysis, 30 μL of the solution of interest was initially added at the extremity of the microfluidic channel (paper) and after 30 s the analysis was performed (time for the solution to travel through the channel). However, all analyses involving CV were performed in static conditions in a 5 mL beaker. For this purpose, the electrode area (9.0 mm²) was delimited using non-conductive colorless enamel, leaving only the working area of the electrodes. Initially, the analysis was carried out with the redox probe FcMeOH (1.0 mmol L⁻¹ in 0.1 mol L⁻¹ KCl), for all analyses carried out with the electrodes before and after surface treatment. For this, an electrochemical treatment previously described in the literature using 0.5 mol L⁻¹ NaOH was employed [25]. Subsequently, the cyclic voltammetry (CV) technique was employed with different scan rates (from 20 to 140 mV s⁻¹) in a potential window from -0.4 to +0.7 V, to obtain the electroactive surface area of the treated and untreated sensors. Then, the cyclic voltammograms for both sensors (treated and untreated) at a scan rate of 50 mV s⁻¹ were also compared. Finally, the treated and untreated sensors were tested in the analysis (using CV) of 1.0 mmol L⁻¹ CBZ in 0.1 mol L⁻¹ BR buffer (pH 4.0). From the results obtained in this step, the treated sensor was chosen as ideal and applied in all subsequent CBZ analyses.

The optimization of the pH of the supporting electrolyte to be used

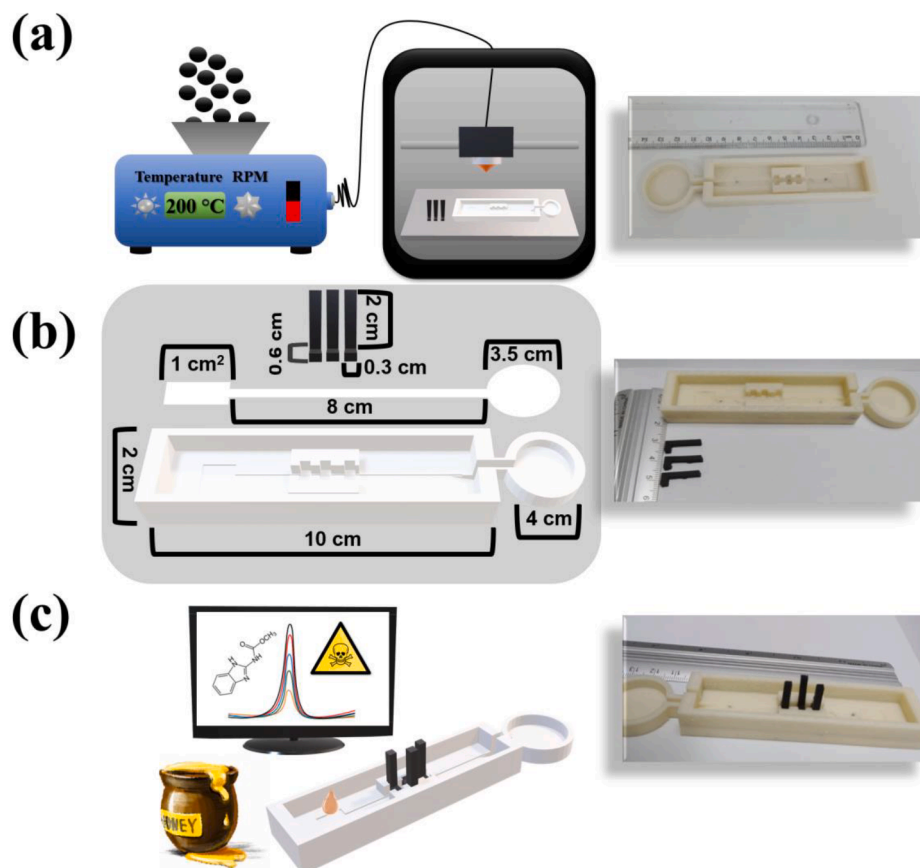


Fig. 1. Illustration of a summary scheme of all the steps involved in this work. (a) Production of conductive filaments with CB/PLA, 3D printing of the microfluidic device based on non-conductive PLA filaments, and electrochemical sensors based on CB/PLA. (b) Structural scheme of the complete microfluidic device, sensors, fluidic paper, and base, with their respective dimensions. (c) Analysis of CBZ in honey from a portable potentiostat and microfluidic device using only a 30 μL drop.

for the analysis of CBZ was also performed. For this, successive tests were carried out using CV with a scan rate of 50.0 mV s^{-1} , in the potential window of $+0.4$ to $+1.4 \text{ V}$, using 0.1 mol L^{-1} BR buffer in the pH range of 2.0 to 6.0. The solution of pH 4.0 was chosen as optimal and used in all subsequent analyses. Then, comparative tests were performed between different voltammetric techniques for CBZ detection, namely differential pulse voltammetry (DPV) and SWV, using both a scan rate of 30.0 mV s^{-1} . The analysis was carried out in the potential range of $+0.6$ to $+1.4 \text{ V}$ using a solution of $30.0 \mu\text{mol L}^{-1}$ CBZ in BR buffer (pH 4.0). SWV was chosen as the ideal technique to perform the quantitative analysis of CBZ based on higher electrochemical response. Therefore, the operational parameters of the SWV technique, step potential, amplitude, and frequency were optimized in the ranges of values studied from 1 to 8 mV, 10 to 90 mV, and 10 to 50 Hz, respectively. All analyses were performed in the potential window of $+0.4$ to $+1.4 \text{ V}$ with a $10.0 \mu\text{mol L}^{-1}$ CBZ solution in 0.1 mol L^{-1} BR buffer (pH 4.0). Thus, the optimal values chosen were 5 mV, 80 mV, and 40 Hz, for step potential, amplitude, and frequency, respectively.

Given the optimized operational parameters of the SWV technique, an analytical curve was built in the concentration range of 0.5 to $40.0 \mu\text{mol L}^{-1}$ CBZ in 0.1 mol L^{-1} BR buffer (pH 4.0). Subsequently, the microfluidic device was used in the analysis of two samples of honey fortified with three different concentrations of CBZ (0.5; 10.0, and $30.0 \mu\text{mol L}^{-1}$). The honey samples were diluted 1:1 in 0.1 mol L^{-1} BR buffer (pH 4.0).

3. Results and discussion

3.1. Morphological and electrochemical characterizations

The morphological structure of untreated and treated 3D-printed CB-PLA electrodes was evaluated by SEM analysis. Fig. 2 presents the images obtained from the surface of the working electrodes before (Fig. 2a) and after (Fig. 2b) the electrochemical treatment using a 0.5 mol L^{-1} NaOH solution, at magnification factors of 4000 (Fig. 2a and b) and 1000x (Fig. 2a' and 2b') for both sensors.

As can be seen, despite the presence of grooves, the untreated electrode shows some smoothness over the surface (Fig. 2a and a'), which can be attributed to the presence of PLA. After electrochemical treatment (Fig. 2b and b'), greater exposure of CB particles occurred. This exposure was provided by the removal of PLA excess from the surface, as previously reported in studies from the literature [10,26], which resulted in the appearance of a greater number of grooves, evidenced at lower magnifications (Fig. a' and b'). This exposure is important for increasing the electrochemical efficiency of the sensor and improving the electron transfer processes. Furthermore, contact angle measurements were performed for both treated and untreated surfaces, to evaluate the hydrophilic character of the electrodes. Fig. S2 shows the obtained images. In the non-treated electrode, the contact angle of the drop was $69.3^\circ \pm 2.8^\circ$, while for the treated electrode was $61.0^\circ \pm 2.1^\circ$. These results demonstrate that both electrodes have predominantly hydrophilic characteristics, however, this character is slightly more evidenced after the surface treatment, through the decrease of contact angle. This phenomenon can be attributed to the greater presence of CB at the surface, which contains oxygenated groups, contributing to the

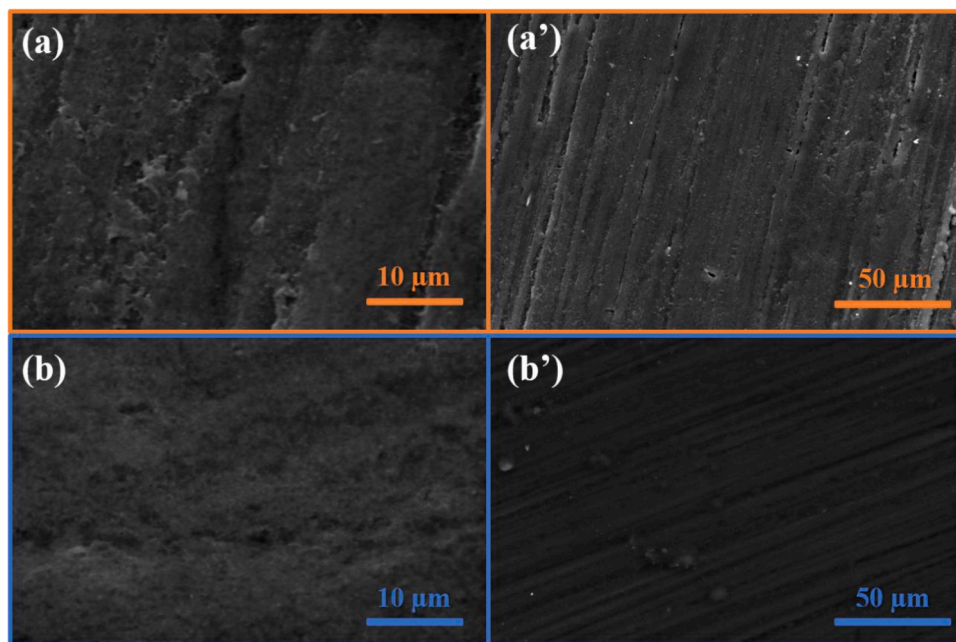


Fig. 2. SEM images of CB-PLA before (a) and after (b) electrochemical surface treatment, at magnifications of 4000 (a and b) and 1000 x (a' and b').

interactions with water, and agrees with previous work from our group described in the literature [10].

The electroactive area of untreated and treated CB-PLA was also

evaluated. For this, CV measurements at different scan rates (20 to 140 mV s^{-1}) were recorded, in presence of 1.0 mmol L^{-1} FcMeOH in 0.1 mol L^{-1} KCl. The electroactive area was estimated following the

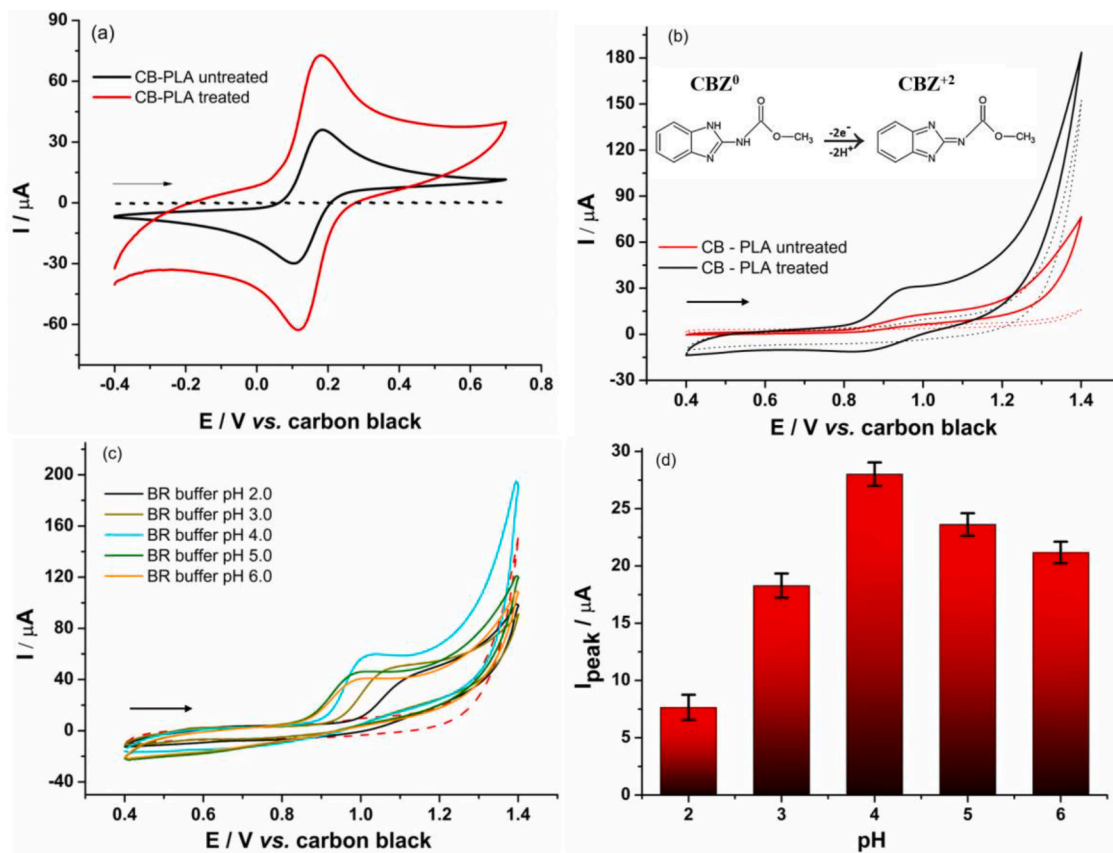


Fig. 3. (a) Comparison between the cyclic voltammograms obtained for 1.0 mmol L^{-1} of FcMeOH in 0.1 mol L^{-1} KCl at CB-PLA electrodes before and after surface treatment; Scan rate: 50 mV s^{-1} ; (b) Cyclic voltammograms obtained for 1.0 mmol L^{-1} CBZ in 0.1 mol L^{-1} BR buffer solution (pH 4.0) at CB-PLA electrodes before and after surface treatment; Inset: mechanism of oxidation of CBZ; Scan rate: 50 mV s^{-1} ; (c) Cyclic voltammograms obtained for 1.0 mmol L^{-1} CBZ in 0.1 mol L^{-1} BR buffer solution at varied pH values, using treated CB-PLA electrode; Scan rate: 50 mV s^{-1} ; (d) Peak current response as a function of pH value.

Randles-Ševčík equation for a quasi-reversible process [26]. Fig. S3 presents the voltammograms obtained for the additive manufactured electrodes and the respective plots of anodic and cathodic peak currents as a function of the square root of the scan rate. The electroactive surface area values obtained for both untreated and treated electrodes were 20.04 and 39.29 mm², respectively. As expected, an increase in the electroactive area value after the surface treatment was observed, corresponding to 2 times in comparison to the untreated surface. This increase confirms the exposure of CB at the electrode surface, showing that the surface treatment was successful. The geometric area of the additive manufactured electrode is 9 mm², this indicates that the calculated electroactive area of the untreated and treated electrodes is 2.3 and 4.4 times larger, respectively. This difference between the geometric and electroactive area can be attributed to the apparent roughness that can be seen in Fig. 2., which is mainly more visible in the treated electrode.

3.2. Voltammetric profile and pH optimization

The voltammetric profile of untreated and treated electrodes was evaluated using the CV technique, in the presence of a 1.0 mmol L⁻¹ FcMeOH redox probe, in 0.1 mol L⁻¹ KCl. As can be seen in Fig. 3a, a peak current of 30.0 μA was obtained for the untreated electrode, while approximately 50.0 μA was observed after surface treatment. As expected, after treatment the current response increased significantly (approximately 67%), evidencing the exposition of conductive material at the electrode surface, which consequently improved the electrode performance, supporting a more efficient analysis. The electrochemical behavior of the analyte of interest (CBZ) was also evaluated. Furthermore, it is worth mentioning that both treated and untreated CB-PLA showed ΔE_p of 0.061 and 0.076 V (Fig. 3a), respectively, demonstrating good reversibility of the system. In this context, even though the treated CB-PLA presented a higher signal intensity than the untreated one, it presented satisfactory electrochemical responses and good resolution of the voltammograms. These excellent characteristics of the sensors can be linked to two factors, the amount of conductive material (28.5%) present in the filament used in the manufacture of the sensor and possibly the length of the electrode connection. According to Crapnell et al., 2022 [27], the shorter the sensor connection length, the better the charge transfer resistance, ΔE_p, and the heterogeneous electron transfer rate constant. Thus, since the present work designed the sensor to occupy the smallest possible space in the microfluidic device, in which the length of the sensor connection was the smallest possible with a size of 20.0 mm, which may have favored the characteristics electrochemical characteristics of the treated and untreated CB-PLA sensor. Fig. 3b shows the voltammetric profile of 1.0 mmol L⁻¹ CBZ in a 0.1 mol L⁻¹ BR buffer (pH 4.0) solution.

In Fig. 3b it is possible to observe that CBZ presented an oxidation peak at the approximate potential of +0.95 V (vs. carbon black – CB-PLA), referring to its oxidation from CBZ⁰ to CBZ²⁺ (mechanism inset), which involves a two-proton and two-electron transfer process [5]. Peak current values of 5.0 and 15.0 μA were obtained for untreated and treated electrodes, respectively. This represents an increase of 3-fold in the peak current after surface treatment. These results demonstrate the importance of electrochemical treatment, as well as its effectiveness.

The optimization of the pH of the supporting electrolyte was carried out using a BR buffer solution in the pH range of 2.0 to 6.0. Fig. 3c presents the voltammograms obtained, and Fig. 3d the respective peak current responses. It can be seen that the peak current increases with the pH value, reaching a maximum at a pH value of 4.0, followed by a decrease at higher pH values. Thus, the BR buffer pH 4.0 was employed for all subsequent analyses. This result is in agreement with the previously reported in the literature [22].

To improve the efficiency in the CBZ analysis, SWV and DPV techniques were evaluated facing CBZ electrochemical response. For this, the voltammograms were recorded at the same scan rate (30 mV s⁻¹) using a solution containing 30 μmol L⁻¹ CBZ. The voltammograms obtained

can be seen in Fig. S4, showing oxidation peaks close to +1.1 V (vs. carbon black – CB-PLA) and showing a higher current response using the SWV technique (1.4 μA) in comparison to DPV (0.9 μA). Therefore, SWV was chosen to perform the quantitative analysis of CBZ.

3.3. Optimization of SWV operating parameters

To obtain the best analytical response for CBZ, the operational parameters of the SWV technique (potential step, amplitude, and frequency) were optimized. Values ranging from 1 to 8 mV, 10 to 90 mV, and 10 to 50 Hz, for step potential, amplitude, and frequency, were evaluated, respectively. All analyses were performed using a 10.0 μmol L⁻¹ CBZ solution in 0.1 mol L⁻¹ BR buffer (pH 4.0). Fig. S5 shows the voltammograms obtained, as well as the respective peak current responses. To choose the optimal values, three features were considered, including higher peak current, voltammogram resolution, and half-peak width.

In Fig. S5a, is possible to observe that all voltammograms presented a good resolution and no significant broadening of the half-peak potential was observed. Thus, the peak current was the determining factor for the choice, and the value of 5 mV was chosen as the optimal step potential value. In Fig. S5b it is possible to observe that as the amplitude increases, the peak current increases proportionally. However, at an amplitude value of 90 mV, there is a substantial increase in the half-peak width, therefore the value of 80 mV was chosen as optimal since it presents a satisfactory peak current value, good resolution, and no considerable peak enlargement. Finally, in Fig. S5c it is possible to observe a similar behavior presented by the optimization of the frequency. Thus, the optimal frequency value was defined based on the highest peak current obtained (40 Hz). Therefore, all subsequent analyses were carried out using the SWV at a step potential of 5 mV, amplitude of 80 mV, and frequency of 40 Hz.

3.4. Analytical curve and determination of CBZ in honey

Using the optimized operational parameters of the SWV, an analytical curve for CBZ in the concentration ranges from 0.5 to 40.0 μmol L⁻¹ was constructed. For this, six additions of increasing concentrations were performed and the voltammograms were recorded in triplicate. At higher concentration values occurred a decrease in the current response, not reaching linearity. To carry out the analysis, a different filter paper (microfluidic channel) was used for each registered concentration. Fig. 4 shows the obtained voltammograms and respective calibration curve.

Linear behavior is observed at CBZ concentrations from 0.5 to 40 μmol L⁻¹, following the equation $I(\mu A) = 1.16 + 0.71 \times C_{CBZ}(\mu mol L^{-1})$, with $R^2 = 0.997$. The sensitivity obtained was 0.71 μA μmol⁻¹ L. From the slope value of the calibration curve (b) and intercept error values, the limits of detection (LOD) and quantification (LOQ) were calculated according to the following: $LOD = (3.3 \times SD_{intercept})/b$ and $LOQ = 3 \times LOD$, where SD is the standard deviation. The calculated LOD and LOQ were 0.09 and 0.31 μmol L⁻¹, respectively.

The repeatability tests were also performed by recording 10 voltammograms in sequence using the same electrode and a CBZ solution of concentration 1.0 μmol L⁻¹, in which the RSD value of 4.65%, was obtained. A reproducibility test was also performed by SWV employing a 1.0 μmol L⁻¹ CBZ solution at four different sensors. An RSD value of 3.81% was obtained, showing good reproducibility between different sensors. The voltammograms recorded for repeatability (Fig. S6a) and reproducibility (Fig. S6b) can be seen in Fig. S6. The results obtained demonstrate that the fluidic device in conjunction with the electrochemical sensors presents an adequate performance in the analysis of CBZ, encompassing the Brazilian legislation for the control of CBZ in honey. Thus, the developed device has great potential to be used as an alternative method of analysis.

From the analytical characteristics obtained in the present work, a comparative analysis was carried out with results from works described

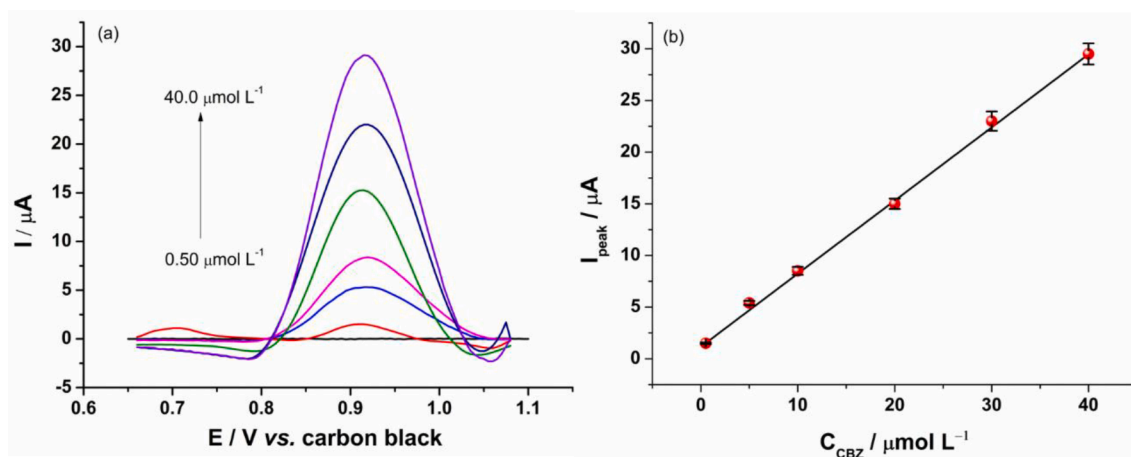


Fig. 4. (a) SWV recordings for increasing concentrations of CBZ (0.5, 5.0, 10.0, 20.0, 30.0, and 40.0 $\mu\text{mol L}^{-1}$) in 0.1 mol L⁻¹ mol L⁻¹ BR buffer (pH 4.0), and (b) respective analytical curve. SWV parameters: 5 mV (step potential); 80 mV (amplitude); 40 Hz (frequency).

in the literature. Table 1 presents the analytical characteristics of several reported articles and the present work.

The literature reports several works using electrochemical sensors related to CBZ detection. To our knowledge, the use of additive-manufactured electrodes for pesticide detection is reported only once in a previous work by our group, in which graphite-based electrodes were used. However, in the present work, an additive-manufactured microfluidic device was used, with a paper-based flow channel and 3D sensors based on CB/PLA. In comparison with the other works presented, it is observed that the calculated LOD are all close to the present work, demonstrating the efficiency of the developed device. Furthermore, this work presents for the first time the use of a microfluidic device for CBZ. Thus, by linking the qualities of 3D printing, low-cost material (carbon black), and the microfluidic device, it is possible to

obtain an additive manufactured microfluidic device for electrochemical detection of CBZ of high quality and great potential, with a result comparable to the sensors already previously reported.

The applicability of the method using the additive manufactured microfluidic device, the analysis of 2 different honey samples (Table 2). Each sample was fortified with three different CBZ concentrations (0.5; 10.0 and 30.0 $\mu\text{mol L}^{-1}$).

The recovery test indicated recovery values ranging from 92.4 to 108.8% for all samples tested. This result indicates that the developed device can be employed in the electrochemical analysis of CBZ in honey with no matrix effect. Thus, the 3D-printed microfluidic device together with electrochemical sensors demonstrates good applicability for monitoring CBZ in honey.

Table 1

Comparison of the analytical characteristics of the proposed method using a 3D microfluidic device with reported in the literature for the determination of CBZ in real samples.

Electrode	Technique	Samples	Linear range ($\mu\text{mol L}^{-1}$)	LOD ($\mu\text{mol L}^{-1}$)	Ref
3D Gpt-PLA ^a	SWV	Honey, Milk, Orange juice, and water	0.5 – 50.0	0.03	[22]
SPCE/K-n ^b SPCE/K-a ^b	DPV	Apple and Cabbage	0.5 – 10.0	0.17 0.06	[21]
SPES ^c	DPV	Wine	0.1 – 1.0	0.06	[20]
QD-GO/ CPE ^d	DPV	Orange juice	0.099 – 11.8	0.092	[17]
NP-Cu/ RGO/ GCE ^e	DPV	Pond water and Lettuce	0.5 – 30.0	0.09	[18]
β -CD- MWCNTs- BDDE ^f	SWAdSV ^h	River water	0.67 – 11.2	0.196	[19]
BDD ^g	SWV	Lemon juice	4.95 – 69.0	1.6	[28]
3D CB-PLA	SWV	Honey	0.5 – 40.0	0.091	This work

^a 3D graphite and polylactic acid electrochemical sensor.

^b screen printed carbon electrode.

^c screen printed electrode made of carbon conductive ink.

^d carbon paste electrodes modified with the nanocomposite.

^e NP-Cu and RGO modified electrode.

^f boron-doped diamond electrode modified with multiwalled carbon nanotubes and β -cyclodextrin.

^g boron-doped diamond.

^h square wave adsorptive stripping voltammetric.

3.5. Amperometric assay

To demonstrate that the proposed 3D-printed microfluidic device can also be used in a full analysis employing a single microfluidic paper, a test with the redox probe FcMeOH was performed on the CB-PLA electrodes before and after treatment. For this, amperometric responses were recorded in triplicate for increasing concentrations (0.01 to 1.00 mmol L⁻¹) of FcMeOH. Fig. 5 presents the amperograms obtained, applying a fixed potential of +0.1 V. Each solution addition was performed after 150 s on a single paper.

As can be seen, amperometric peaks were observed due to the fluidic path of the solutions containing FcMeOH through the filter paper. With this, it is possible to observe that both electrodes (untreated and treated) presented increasing peak current responses as the concentration increased. However, for the untreated electrode, the current responses were much lower and did not show a linear response in the proposed range. On the other hand, the treated sensor showed a linear response for the concentration range of 0.01 to 1.00 mmol L⁻¹ FcMeOH, with an $R^2 = 0.998$. Thereby, the quantification using this technique is possible using a single filter paper. This result demonstrates that the fluidic

Table 2

CBZ concentrations and recovery values obtained from the microfluidic device, and printed electrode in additive-manufactured CB-PLA.

Sample	Spiked ($\mu\text{mol L}^{-1}$)	Found ($\mu\text{mol L}^{-1}$)	Recovery (%)
Wild honey	0.50	0.52 \pm 0.03	104.0 \pm 6.0
	10.0	9.32 \pm 0.52	93.2 \pm 5.2
	30.0	31.4 \pm 1.2	104.7 \pm 4.0
Jatai honey	0.50	0.54 \pm 0.02	108.0 \pm 4.0
	10.0	10.6 \pm 0.5	106.0 \pm 5.1
	30.0	30.2 \pm 1.8	100.6 \pm 6.0

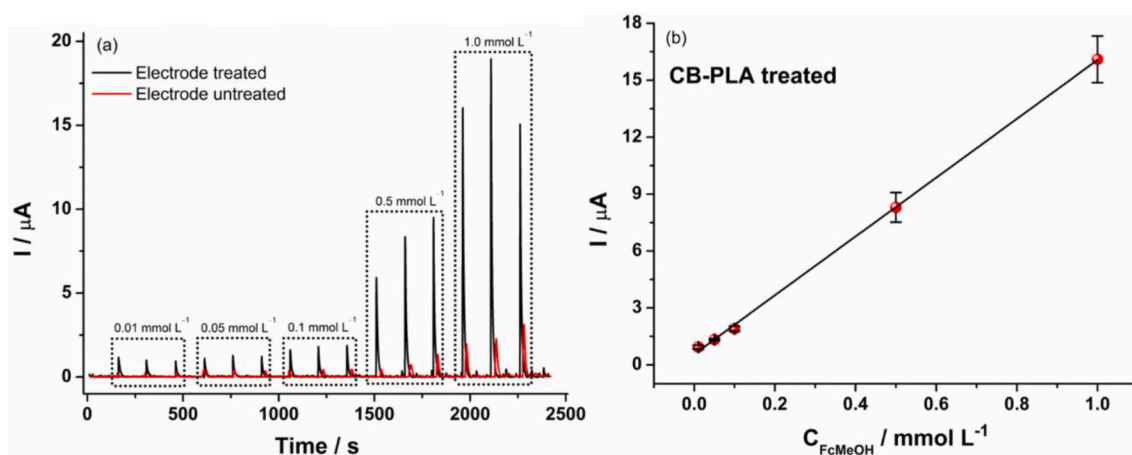


Fig. 5. (a) Amperograms recorded for increasing concentrations of FcMeOH (0.01, 0.05, 0.1, 0.5, and 1.0 mmol L⁻¹). Working potential: +0.1 V.

device has great potential for application in constant flow analysis, demonstrating that additive manufactured devices can be applied successfully in different analytical ways and for different purposes.

4. Conclusion

A 3D-printed microfluidic device in conjunction with filter paper for the electrochemical detection of CBZ was successfully obtained. The use of 3D printing technology, together with sustainable and renewable materials such as PLA and paper, is highly important to contribute to green chemistry. The electrochemical analysis of CBZ presented satisfactory results with a low LOD (0.91 $\mu\text{mol L}^{-1}$) that meets the requirements of the Brazilian legislation for analysis in honey. The recovery test performed in two different types of honey showed recovery results ranging from 92.4 to 108.8%, demonstrating the efficiency of the developed device. In addition, it was possible to demonstrate that the device can be used to perform flow amperometric analysis, indicating the versatility of the 3D microfluidic platform. Thus, the construction of an additive-manufactured microfluidic device demonstrates the high versatility of 3D printing for analytical chemistry, being able to build a microfluidic platform and electrochemical sensors. In addition, the device is portable and requires minimal amounts of samples to perform the analysis. Together with portable equipment, it is possible to carry out analysis in loco, bringing cost reduction and practicality for the operator.

Declaration of Competing Interest

The authors declare that they have no known competing financial interests or personal relationships that could have appeared to influence the work reported in this paper.

Acknowledgments

The authors are grateful to the Brazilian agencies FAPESP (2017/21097-3, 2022/06145-0), CAPES (001; 88887.504861/2020-00) CNPq (303338/2019-9; 380632/2023-3).

Supplementary materials

Supplementary material associated with this article can be found, in the online version, at doi:10.1016/j.talo.2023.100213.

References

- [1] S. Singh, N. Singh, V. Kumar, S. Datta, A.B. Wani, D. Singh, K. Singh, J. Singh, Toxicity, monitoring and biodegradation of the fungicide carbendazim, *Environ. Chem. Lett.* 14 (2016) 317–329.
- [2] S. Boudh, J.S. Singh, Pesticide Contamination: Environmental Problems and Remediation Strategies, in: *Emerg. Eco-Friendly Approaches Waste Manag.*, Springer, Singapore, 2018, pp. 245–269.
- [3] W.H. Goodson, et al., Assessing the carcinogenic potential of low-dose exposures to chemical mixtures in the environment: the challenge ahead, *Carcinogenesis* 36 (2015) S254–S296.
- [4] A.L.G. Ferreira, S. Loureiro, A.M.V.M. Soares, Toxicity prediction of binary combinations of cadmium, carbendazim and low dissolved oxygen on *Daphnia magna*, *Aquat. Toxicol.* 89 (2008) 28–39.
- [5] A. Özcan, F. Hamid, A.A. Özcan, Synthesizing of a nanocomposite based on the formation of silver nanoparticles on fumed silica to develop an electrochemical sensor for carbendazim detection, *Talanta* 222 (2021).
- [6] Ministério da Saúde, (2002). https://bvsms.saude.gov.br/bvs/saudelegis/anvisa/2002/rdc0347_16_12_2002.html (accessed November 12, 2022).
- [7] A. Ambrosi, M. Pumera, 3D-printing technologies for electrochemical applications, *Chem. Soc. Rev.* 45 (2016) 2740–2755.
- [8] E.M. Richter, D.P. Rocha, R.M. Cardoso, E.M. Keefe, C.W. Foster, R.A.A. Munoz, C. E. Banks, Complete additively manufactured (3D-Printed) electrochemical sensing platform, *Anal. Chem.* 91 (2019) 12844–12851.
- [9] J.S. Stefano, L.O. Orzari, H.A. Silva-Neto, V.N. de Ataíde, L.F. Mendes, W.K. T. Coltro, T.R. Longo Cesar Paixão, B.C. Janegitz, Different approaches for fabrication of low-cost electrochemical sensors, *Curr. Opin. Electrochem.* 32 (2022), 100893.
- [10] J.S. Stefano, L.R.G.E. Silva, B.C. Janegitz, New carbon black-based conductive filaments for the additive manufacture of improved electrochemical sensors by fused deposition modeling, *Mikrochim. Acta* 189 (2022) 414.
- [11] J.S. Stefano, C. Kalinke, R.G. da Rocha, D.P. Rocha, V.A.O.P. da Silva, J.A. Bonacin, L. Angnes, E.M. Richter, B.C. Janegitz, R.A.A. Muñoz, Electrochemical (Bio)sensors enabled by fused deposition modeling-based 3D printing: a guide to selecting designs, printing parameters, and post-treatment protocols, *Anal. Chem.* (2022) acs.analchem.1c05523.
- [12] E. Sigley, C. Kalinke, R.D. Crapnell, M.J. Whittingham, R.J. Williams, E.M. Keefe, B.C. Janegitz, J.A. Bonacin, C.E. Banks, Circular economy electrochemistry: creating additive manufacturing feedstocks for caffeine detection from post-industrial coffee pod waste, *ACS Sustain. Chem. Eng.* (2023).
- [13] R.M. Cardoso, C. Kalinke, R.G. Rocha, P.L. dos Santos, D.P. Rocha, P.R. Oliveira, B. C. Janegitz, J.A. Bonacin, E.M. Richter, R.A.A. Munoz, Additive-manufactured (3D-printed) electrochemical sensors: a critical review, *Anal. Chim. Acta* 1118 (2020) 73–91.
- [14] H.A. Silva-Neto, I.V.S. Arantes, A.L. Ferreira, G.H.M. do Nascimento, G.N. Meloni, W.R. de Araujo, T.R.L.C. Paixão, W.K.T. Coltro, Recent advances on paper-based microfluidic devices for bioanalysis, *TrAC Trends Anal. Chem.* 158 (2023), 116893.
- [15] I.V.S. Arantes, T.R.L.C. Paixão, Couple batch-injection analysis and microfluidic paper-based analytical device: a simple and disposable alternative to conventional BIA apparatus, *Talanta* 240 (2022), 123201.
- [16] V.A.O.P. da Silva, R.C. de Freitas, P.R. de Oliveira, R.C. Moreira, L.H. Marcolino-Júnior, M.F. Bergamini, W.K.T. Coltro, B.C. Janegitz, Microfluidic paper-based device integrated with smartphone for point-of-use colorimetric monitoring of water quality index, *Measurement* 164 (2020), 108085.
- [17] P.C.A. Santana, J.B.S. Lima, T.B.S. Santana, L.F.S. Santos, C.R.S. Matos, L.P. da Costa, I.F. Gimenez, E.M. Sussuchi, Semiconductor nanocrystals-reduced graphene composites for the electrochemical detection of carbendazim, *J. Braz. Chem. Soc.* 30 (2019) 1302–1308.
- [18] C. Tian, S. Zhang, H. Wang, C. Chen, Z. Han, M. Chen, Y. Zhu, R. Cui, G. Zhang, Three-dimensional nanoporous copper and reduced graphene oxide composites as

- enhanced sensing platform for electrochemical detection of carbendazim, *J. Electroanal. Chem.* 847 (2019), 113243.
- [19] M. Brycht, O. Vajdle, K. Sipa, J. Robak, K. Rudnicki, J. Piechocka, A. Tasić, S. Skrzypek, V. Guzsvány, B-Cyclodextrin and multiwalled carbon nanotubes modified boron-doped diamond electrode for voltammetric assay of carbendazim and its corrosion inhibition behavior on stainless steel, *Ionics (Kiel)* 24 (2018) 923–934.
- [20] P.A. Raymundo-Pereira, N.O. Gomes, J.H.S. Carvalho, S.A.S. Machado, O. N. Oliveira, B.C. Janegitz, Simultaneous detection of quercetin and carbendazim in wine samples using disposable electrochemical sensors, *ChemElectroChem* 7 (2020) 3074–3081.
- [21] T.S. Martins, S.A.S. Machado, O.N. Oliveira, J.L. Bott-Neto, Optimized paper-based electrochemical sensors treated in acidic media to detect carbendazim on the skin of apple and cabbage, *Food Chem.* 410 (2023), 135429.
- [22] L.R. Guterres Silva, J. Santos Stefano, R. Cornélio Ferreira Nocelli, B. Campos Janegitz, 3D electrochemical device obtained by additive manufacturing for sequential determination of paraquat and carbendazim in food samples, *Food Chem.* 406 (2023), 135038.
- [23] V.A.O.P. da Silva, V.A.P. Tartare, C. Kalinke, P.R. de Oliveira, D.C. de Souza, J. A. Bonacin, B.C. Janegitz, Lab-made 3D-printed contact angle measurement adjustable holder, *Quim. Nova.* 43 (2020) 1312–1319.
- [24] J.S. Stefano, L.R. Guterres e Silva, R.G. Rocha, L.C. Brazaca, E.M. Richter, R. A. Abarza Muñoz, B.C. Janegitz, New conductive filament ready-to-use for 3D-printing electrochemical (bio)sensors: towards the detection of SARS-CoV-2, *Anal. Chim. Acta.* (2021), 339372.
- [25] R.M. Cardoso, D.M.H. Mendonça, W.P. Silva, M.N.T. Silva, E. Nossol, R.A.B. da Silva, E.M. Richter, R.A.A. Muñoz, 3D printing for electroanalysis: from multiuse electrochemical cells to sensors, *Anal. Chim. Acta.* 1033 (2018) 49–57.
- [26] A.G.M. Ferrari, C.W. Foster, P.J. Kelly, D.A.C. Brownson, C.E. Banks, Determination of the electrochemical area of screen-printed electrochemical sensing platforms, *Biosensors* 8 (2018) 1–10.
- [27] R.D. Crapnell, A. Garcia-Miranda Ferrari, M.J. Whittingham, E. Sigley, N.J. Hurst, E.M. Keefe, C.E. Banks, Adjusting the connection length of additively manufactured electrodes changes the electrochemical and electroanalytical performance, *Sensors* 22 (2022) 9521. Page22 (2022) 9521.
- [28] T. Lima, H.T.D. Silva, G. Labuto, F.R. Simões, L. Codognoto, An experimental design for simultaneous determination of carbendazim and fenamiphos by electrochemical method, *Electroanalysis* 28 (2016) 817–822.